



THE UNIVERSITY
of EDINBURGH



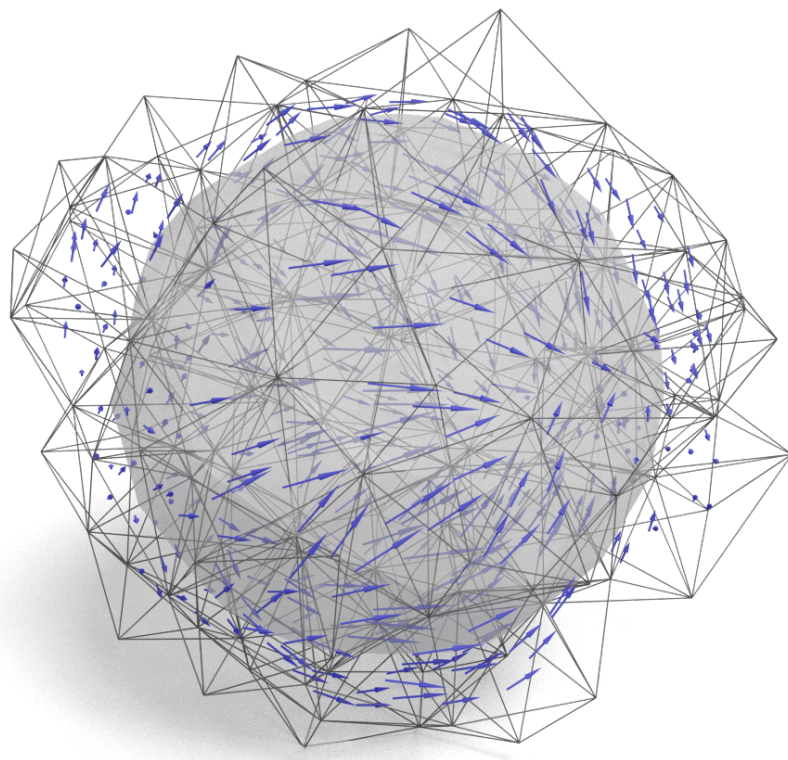
Internship report

VECTOR-FIELD DESIGN ON IMPLICIT SDFs

Mattéo Clémot

Supervised by Amir Vaxman
(The Institute of Perception, Action and Behaviour)

February – July 2023



Contents

1	Helmholtz-Hodge decomposition for explicit spaces	3
1.1	Explicit operators	3
1.2	Helmholtz decomposition	4
1.3	Dimensionality and topology	5
1.4	Least-square formulation	5
2	Helmholtz-Hodge decomposition for implicit spaces	7
2.1	Operators	7
2.2	Dimensionality and topology	9
2.3	Decomposition	9
2.3.1	Curl-free part	9
2.3.2	Divergence-free part	10
2.3.3	Harmonic part	11
2.4	Robustness	12
2.5	Results	12

Introduction

Context

Tangent vector fields on three-dimensional surfaces are useful in a number of applications, from computer graphics to PDE resolution. One of the main tool to study them is a fundamental theorem known as Helmholtz's theorem, which states that such a vector field can be decomposed as the sum of three components: an irrotational – or curl-free – vector field that writes as the gradient of a scalar field (the potential); a solenoidal – or divergence-free – vector field that writes as the rotated gradient of another scalar field; and a harmonic vector field, both curl-free and divergent-free, that depends on the topology of the surface. It is known how to perform an algebraically robust decomposition on a triangular mesh (in particular such that the harmonic space has the correct dimension given the topology of the surface).

Objective

During this internship, we were interested in tangent vector fields on implicit surfaces which are given by the level sets of some differentiable function ϕ . The aim was to explore the possibility to perform a Helmholtz-Hodge decomposition on level sets of a given implicit function, in an algebraically and topologically robust way.

Plan

In Section 1, we introduce differential operators on a triangular mesh and how it is possible to perform a robust Helmholtz-Hodge decomposition on it.

In Section 2, we introduce the differential operators we used in the implicit setting, and we present a method on which we worked in order to perform the decomposition on level sets, based on the extrapolation from a single level set.

Code

The implementation was made in Python and is available at the following repository:

https://github.com/MClemot/Implicit_HHD

It has the following dependencies:

- bpy and BlenderToolBox for Blender renderings;
- Gudhi for the simplicial complex representation;
- IGL for geometry processing;
- Polyscope for visualisation;
- SciPy for linear algebra and sparse matrices;
- TetGen for tetrahedral mesh generation.

1 Helmholtz-Hodge decomposition for explicit spaces

In this section we present how to perform a vector field decomposition on a triangular mesh in a algebraically robust way. The method was introduced in [PP03]. We rely on the definitions of [BV22] and [DGDT16]. In the entire section, we are working with explicit surfaces given by a mesh $\mathcal{M} = (\mathcal{V}, \mathcal{E}, \mathcal{F})$ where $\mathcal{V} \subset \mathbb{R}^3$ is a finite set of vertices, $\mathcal{E} \subset \mathcal{V}^2$ the set of edges and $\mathcal{F} \subset \mathcal{P}(\mathcal{V})$ the set of faces. We write $S = \bigcup_{f \in \mathcal{F}} \text{Conv } f$ the surface represented by \mathcal{M} . We make the additional hypothesis that our mesh is a triangular mesh, that is that all faces are triangles (i.e. $\mathcal{F} \subset \mathcal{V}^3$).

In Section 1.1 we first define the classical differential operators: the gradient (∇), the curl ($\nabla \times$) – that we identify to a $\pi/2$ -rotated gradient $J\nabla$, see below – and the divergence ($\nabla \cdot$). We want to define them in a robust way, guaranteeing some structural identities, namely:

$$\begin{aligned}\nabla \times \nabla &= 0 && \text{(curl of gradient is zero)} \\ \nabla \cdot (J\nabla) &= 0 && \text{(divergence of curl/rotated gradient is zero)}\end{aligned}$$

Then we explain how to perform a Helmholtz-Hodge decomposition (Section 1.2) and why it is algebraically robust and how it is related to the topology of the surface (Section 1.3).

1.1 Explicit operators

Scalar and vector fields can be defined over any of the primitives of the mesh: over vertices \mathcal{V} , over edges \mathcal{E} or over faces \mathcal{F} . This choice is important because it changes the dimension of the associated vector space. By abuse of notation we write $d\mathcal{P}$ the vector space $(\mathbb{R}^d)^{\mathcal{P}}$ where \mathcal{P} is either \mathcal{V} , \mathcal{E} or \mathcal{F} . In this section we work with face-based tangent vector fields, and we write $\mathcal{X} = 2\mathcal{F} = (\mathbb{R}^2)^{\mathcal{F}}$ the associated space, whose dimension is $2|\mathcal{F}|$. We will also use vertex-based and edge-based scalar fields (respectively written, by abuse of notation again, \mathcal{V} and \mathcal{E}).

Scalar product between vector fields We first need to define a scalar product between face-based tangent vector fields in \mathcal{X} :

$$\begin{aligned}\langle u, v \rangle &= \int_S u \cdot v \\ &= u^\top M_{\mathcal{X}} v\end{aligned}$$

where $M_{\mathcal{X}} \in \mathbb{R}^{2|\mathcal{F}| \times 2|\mathcal{F}|}$ is the mass matrix, that is a diagonal matrix giving the area of the faces with 2×2 blocks.

Gradient We define the gradient $G_{\mathcal{V}} : \mathcal{V} \rightarrow \mathcal{X}$ as an operator sending a vertex-based scalar field f to a face-based vector field, using the gradients of the basis functions $B_{v,t}, v \in \mathcal{V}, t \in \mathcal{F}$ which are defined as being linear on each triangle t with $B_{v,t}(w) = \begin{cases} 1 & \text{if } w = v \\ 0 & \text{if } w \in t \setminus \{v\} \end{cases}$. For any triangle $t = (i, j, k)$, the gradient of f is:

$$(G_{\mathcal{V}}f)_t = \sum_{v \in \{i, j, k\}} f_v \nabla B_{v,t} \quad \text{with} \quad \nabla B_{i,t} = \frac{1}{2a_t} n_t \times e_{jk}$$

where a_t and n_t are respectively the area and the normal of triangle t .

Divergence The divergence operator is defined as the adjoint of the gradient, that is that we should have for all scalar field f and vector field u :

$$\langle \nabla f, u \rangle = \langle \nabla \cdot u, f \rangle$$

So we want our operator $D : \mathcal{X} \rightarrow \mathcal{V}$ to be such that for any f and u :

$$\begin{aligned}\langle G_{\mathcal{V}}f, u \rangle &= \langle f, Du \rangle \\ f^\top G_{\mathcal{V}}^\top M_{\mathcal{X}} u &= f^\top Du\end{aligned}$$

which requires $D = G_{\mathcal{V}}^\top M_{\mathcal{X}}$.

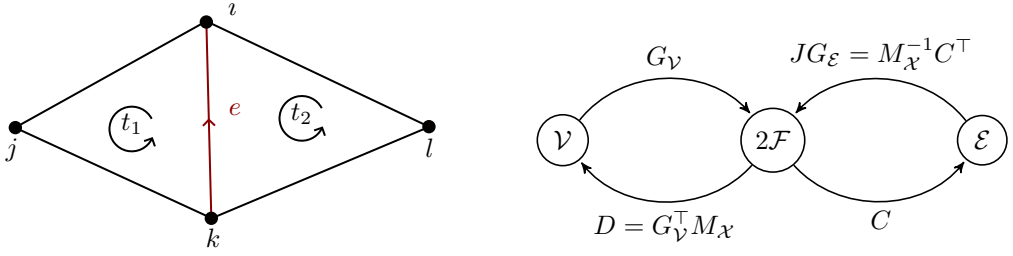


Figure 1: Left: Definition of the curl operator. Right: Summary of the operators between field spaces.

Curl We define the curl operator $C : \mathcal{X} \rightarrow \mathcal{E}$ sending a (face-based) vector field to an edge-based scalar field as follows. For two triangles $t_1 = ijk$ and $t_2 = kli$ sharing the edge $e = ki$ (t_1 is the triangle on the "left" of e and t_2 the one on the "right", see Figure 4, left), we have:

$$\begin{aligned} (Cv)|_e &= \iint_{t_1 \cup t_2} (\nabla \times v) \cdot dS \\ &= \oint_{\partial(t_1 \cup t_2)} v \cdot d\ell \quad (\text{Stokes' theorem}) \\ &= \sum_{e' \in \partial(t_1 \cup t_2)} v \cdot e' \\ &= (v_{t_1} - v_{t_2}) \cdot e \end{aligned}$$

Because the gradient is tangent-continuous across any edge, this definition provides directly the structural identity $CG_{\mathcal{V}} = 0$ (i.e. a gradient field is curl-free).

Rotated gradient We eventually define what we call the rotated gradient operator $JG_{\mathcal{E}} : \mathcal{E} \rightarrow \mathcal{X}$ as the adjoint of the curl, that is that we want that for every edge-based scalar field g and face-based vector field u :

$$\begin{aligned} \langle JG_{\mathcal{E}} g, u \rangle &= \langle g, Cu \rangle \\ g^{\top} JG_E^{\top} u &= g^{\top} M_{\mathcal{X}} C u \end{aligned}$$

which requires $JG_{\mathcal{E}} = M_{\mathcal{X}}^{-1} C^{\top}$. We notice that this provides the second structural identity (i.e. a rotated gradient field is divergence-free) since:

$$DJG_{\mathcal{E}} = G_{\mathcal{V}}^{\top} M_{\mathcal{X}} M_{\mathcal{X}}^{-1} C^{\top} = (CG_{\mathcal{V}})^{\top} = 0.$$

Remark. The rotated gradient can be equivalently defined more directly, as the product of J with $G_{\mathcal{E}}$, where $G_{\mathcal{E}}$ is the midedge-based gradient and J the matrix comprising 2×2 blocks of rotation matrices of angle $\pi/2$ with respect to the surface's normal, allowing to define the curl as the adjoint of this rotated gradient. We can check that these two definitions coincide, which explain why we identify the curl and the rotated gradient, and why we use the notation $JG_{\mathcal{E}}$. However, it is specific to this two-dimensional and linear setting.

See Figure 4 for a summary of the spaces and operators defined above.

1.2 Helmholtz decomposition

In a general setting, the Helmholtz-Hodge theorem states that a vector field v can be decomposed into a sum

$$v = \nabla f + \nabla \times g + h.$$

where the gradient field ∇f is curl-free, the rotated gradient $\nabla \times g$ is divergence-free, and the harmonic field h is both curl-free and divergence-free.

Back to our discrete setting, we want to decompose a face-based vector field $v \in 2\mathcal{T}$ into the following sum, where $f \in \mathcal{V}$ is vertex-based, $g \in \mathcal{E}$ is edge-based and $h \in \ker H$ is harmonic:

$$v = G_{\mathcal{V}}f + JG_{\mathcal{E}}g + h.$$

We define the harmonic operator so that the nullspace $\ker H = \ker D \cap \ker C$ is the harmonic space of the surface:

$$H = \begin{pmatrix} D \\ C \end{pmatrix} : 2\mathcal{F} \rightarrow \mathcal{V} \oplus \mathcal{E}$$

Using the structural identities $CG_{\mathcal{V}} = 0$ and $DJG_{\mathcal{E}} = 0$, we find that we can get the scalar fields f and g by solving the following Poisson systems:

$$\underbrace{G_{\mathcal{V}}^{\top} M_{\mathcal{X}} G_{\mathcal{V}}}_{{\mathcal{L}}_{\mathcal{V}}} f = Dv$$

$$\underbrace{CM_{\mathcal{X}}^{-1} C^{\top}}_{{\mathcal{L}}_{\mathcal{E}}} g = Cv$$

and finally, the harmonic remainder is recovered as $h = v - G_{\mathcal{V}}f - JG_{\mathcal{E}}g$. See Figure 2 for the visualisation of the different parts of the decomposition on two different surfaces.

1.3 Dimensionality and topology

We explain here why choosing the divergence to be towards vertex-based scalar fields and the curl being towards edge-based scalar fields is essential to guarantee the unicity of this discrete Helmholtz-Hodge decomposition and its algebraic robustness.

Topology of the surface The Euler characteristic, defined for a surface mesh as $\chi = |\mathcal{V}| - |\mathcal{E}| + |\mathcal{F}|$ provides a topological invariant. For a closed orientable surface, the Euler characteristic is related to the genus g (intuitively, the number of "handles" in the surface) with the relation $\chi = 2 - 2g$. For instance a sphere is a 0-genus surface, while a torus is a 1-genus surface. The fertility statue depicted in Figure 2 is a 4-genus surface, and the "tetrahedron wireframe" surface shown in Figure ?? is a 3-genus surface.

As we are working with a triangular mesh, we also have $3|\mathcal{F}| = 2|\mathcal{E}|$ (because each face is bounded by three edges and each edge in the intersection of two faces). This can combined with the equality $|\mathcal{V}| - |\mathcal{E}| + |\mathcal{F}| = 2 - 2g$ to obtain the identity

$$2|\mathcal{F}| = |\mathcal{E}| + |\mathcal{V}| + 2g - 2.$$

Dimensionality The rank of the gradient $G_{\mathcal{V}}$ is $|\mathcal{V}| - 1$ (the kernel is the constant scalar functions), and similarly the rank of the rotated gradient $JG_{\mathcal{E}}$ is $|\mathcal{E}| - 1$. In addition, the dimension of face-based tangent vector fields is $2|\mathcal{F}|$. Thanks to the structural identities we can show that

$$\underbrace{2\mathcal{F}}_{2|\mathcal{F}|} = \underbrace{\text{Im } G_{\mathcal{V}}}_{|\mathcal{V}|-1} \oplus \underbrace{\text{Im } JG_{\mathcal{E}}}_{|\mathcal{E}|-1} \oplus \underbrace{\ker H}_{2g}$$

which gives the unicity of the Helmholtz-Hodge decomposition in this discrete setting and the fact that the harmonic space has the correct dimension $2g$. In particular, the harmonic space is null for a 0-genus surface, e.g. a sphere (i.e. on a sphere, the harmonic part of the decomposition is always null). On a 1-genus torus, the harmonic space is of dimension 2 (see Figure 2).

1.4 Least-square formulation

We can also see the curl-free part (respectively divergence-free part, harmonic part) of the Helmholtz decomposition as the closest function to v – in the least squares sense – that writes as a gradient field (respectively as a rotated gradient field, as a harmonic function). This perspective will be useful in the next section.

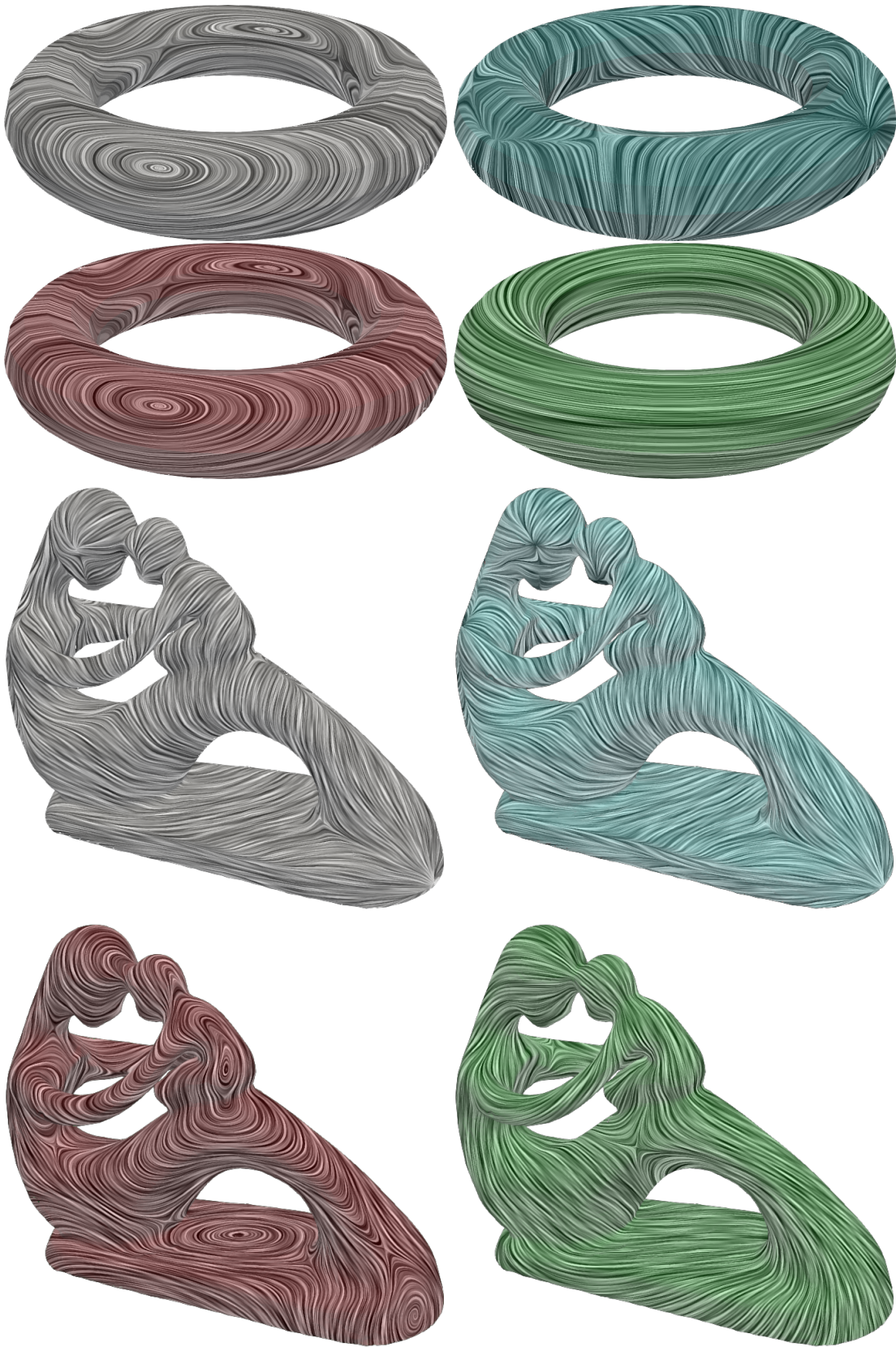


Figure 2: Visualization of the direction of the different terms in the Helmholtz decomposition of a vector field on a 1-genus torus (top) and a 4-genus surface (bottom). The input v is in black, the curl-free part $G_V f$ is in blue, the divergence-free part $JG_E g$ is in red, and harmonic remainder part is in green. The pictures were made using the Line Integral Convolution (LIC) method [CL93] with the scientific visualization software ParaView.

Indeed, the solution f^* to the following least-squares problem $\arg \min_f \|\sqrt{M_{\mathcal{X}}}(G_{\mathcal{V}} f - v)\|_2$ is such that

$$\begin{aligned} (G_{\mathcal{V}}^\top \sqrt{M_{\mathcal{X}}} \sqrt{M_{\mathcal{X}}} G_{\mathcal{V}}) f^* &= G_{\mathcal{V}}^\top \sqrt{M_{\mathcal{X}}} \sqrt{M_{\mathcal{X}}} v \\ \mathcal{L}_{\mathcal{V}} f^* &= Dv \end{aligned}$$

which is exactly the Poisson system expressed in Section 1.2. Similarly, the least-square solution g^* to $\arg \min_g \|\sqrt{M_{\mathcal{X}}}(JG_{\mathcal{E}} g - v)\|_2$ is such that $\mathcal{L}_{\mathcal{E}} g^* = Cv$.

Finally, the solution h^* to the linearly constrained least-square problem

$$\begin{aligned} \arg \min_h \quad & \|\sqrt{M_{\mathcal{X}}}(h - v)\|_2 \\ \text{s.t.} \quad & Hh = 0 \end{aligned}$$

is exactly the remainder as expressed in Section 1.2 (see [Ame85] for the expression of the solution of a linearly constrained least-square problem):

$$\begin{aligned} h^* &= v - M_{\mathcal{X}}^{-1} H^\top (H M_{\mathcal{X}}^{-1} H^\top)^{-1} H v \\ &= v - M_{\mathcal{X}}^{-1} (D^\top \quad C^\top) \begin{pmatrix} \mathcal{L}_{\mathcal{V}}^{-1} & 0 \\ 0 & \mathcal{L}_{\mathcal{E}}^{-1} \end{pmatrix} \begin{pmatrix} D \\ C \end{pmatrix} v \\ &= v - G_{\mathcal{V}} \underbrace{\mathcal{L}_{\mathcal{V}}^{-1} D v}_{f^*} - JG_{\mathcal{E}} \underbrace{\mathcal{L}_{\mathcal{E}}^{-1} C v}_{g^*} \end{aligned}$$

2 Helmholtz-Hodge decomposition for implicit spaces

In this section we explain what we explored during the internship. Instead of having an explicit surface (e.g. a triangular mesh) on which we consider vector fields, we rather work with implicit surfaces. More precisely, we have a differentiable function $\phi : \mathbb{R}^3 \rightarrow \mathbb{R}$ whose level sets $S_\ell = \{\mathbf{x} \mid \phi(\mathbf{x}) = \ell\}$ are isosurfaces. For example, the implicit function given by $\phi(\mathbf{x}) = \|\mathbf{x}\| - r$ gives spheres as level sets. The gradient $\nabla \phi$ gives the normal to the surface.

In this section, we work with several types of vector fields:

- vector fields in the ambient space \mathbb{R}^3 ;
- vector fields on an isosurface S_ℓ ;
- tangential vector fields on an isosurface S_ℓ (for all $x \in L_\ell$, $v(x) \cdot \nabla \phi(x) = 0$).

In a discrete point of view, we consider an ambient tetrahedral mesh $\mathcal{M} = (\mathcal{V}, \mathcal{E}, \mathcal{F}, \mathcal{T})$ (respectively, the vertices, the edges, the faces and the tetrahedra). ϕ is given as a scalar function on \mathcal{V} , that gives a normal $\nabla \phi$ on each $t \in \mathcal{T}$ (i.e. ϕ is piecewise linear on the tetrahedra and $\nabla \phi$ is piecewise constant on the tetrahedra). We also set a triangular mesh $\mathcal{M}^0 = (\mathcal{V}^0, \mathcal{E}^0, \mathcal{F}^0)$ approximating the 0 level set S_0 of ϕ .

In Section 2.1, we first define some new operators for this implicit surfaces setting. In Section 2.2, we highlight the fact that we cannot guarantee the robustness the same way than in the triangular mesh setting. We then construct a method to compute the different parts of the Helmholtz-Hodge decomposition (Sections 2.3.1, 2.3.2, 2.3.3). We argue its algebraic robustness in Section 2.4 and show some results in Section 2.5.

2.1 Operators

Gradient and projected gradient The gradient operator G is defined more or less in the same way as in Section 1.1, i.e. as the sum of the gradient of the basis functions. For any tetrahedron $t = (i, j, k, l)$

$$(Gf)_t = \sum_{v \in \{i, j, k, l\}} f_v \nabla B_{v,t} \quad \text{with} \quad \nabla B_{i,t} = \frac{1}{6v_t} n_{(j,k,l)}$$

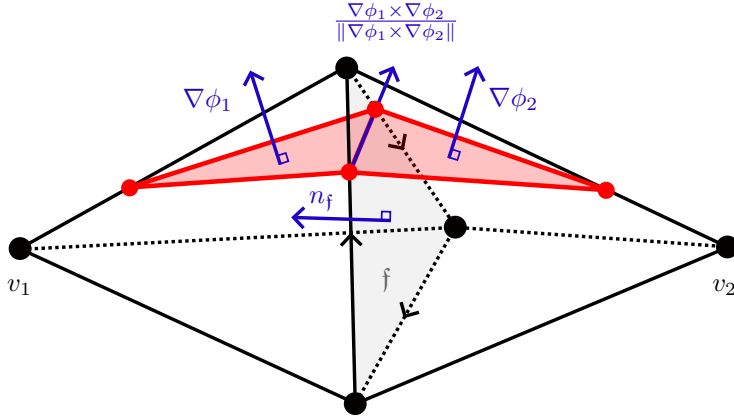


Figure 3: Illustration of the definition of the curl relative to ϕ .

where v_t is the volume of the tetrahedron t and $n_{j,k,l}$ is the normal to the triangle (j, k, l) . The expression is similar for the basis functions.

We also need the projected (onto the level sets) gradient $G_\phi = \Pi_\phi G$ which is given by:

$$(G_\phi f)_t = (Gf)_t - \langle (Gf)_t, (\nabla\phi)_t \rangle (\nabla\phi)_t$$

By design, $(G_\phi f)$ is a ϕ -tangential vector field.

3D curl and tangential curl We can define a 3D curl operator $C_3 : 3\mathcal{T} \rightarrow 3\mathcal{F}^i$ similarly to how we defined C in Section 1.1 (see Figure 3 for notations):

$$\begin{aligned} (C_3 \cdot v)|_f &= \iiint_{t_1 \cup t_2} (\nabla \times v) dV \\ &= - \oint_{\partial(t_1 \cup t_2)} v \times dS \quad (\text{Stokes' theorem}) \\ &= |f|(v_1 - v_2) \times n_f \quad \text{where } n_f \text{ is the normal of the face } f \end{aligned}$$

We also need to define the following tangential curl operator C_ϕ relative to ϕ , based on finite volumes, such that by design, $M_\chi^{-1} C_\phi^\top g$ is a tangential vector field (see Figure 3 for notations):

$$(C_\phi \cdot v)|_f = |f| \left((v_1 - v_2) \cdot \frac{\nabla\phi_1 \times \nabla\phi_2}{\|\nabla\phi_1 \times \nabla\phi_2\|} \right)$$

Orthogonality We can check that we have the structure preservation with the projected gradient G_ϕ , i.e. that:

$$C_\phi \cdot G_\phi = 0.$$

Indeed if $v = G_\phi f = \Pi_\phi \underbrace{Gf}_u$ for some f , then we have on each face f :

$$\begin{aligned} (C_\phi \cdot v)|_f &= |f| ((v_1 - v_2) \cdot t) \text{ with } t = \frac{\nabla\phi_1 \times \nabla\phi_2}{\|\nabla\phi_1 \times \nabla\phi_2\|} \\ &= |f| ((u_1 - (u_1 \cdot n_1)n_1 - u_2 + (u_2 \cdot n_2)n_2) \cdot t) \text{ with } n_1 = \frac{\nabla\phi_1}{\|\nabla\phi_1\|} \text{ and } n_2 = \frac{\nabla\phi_2}{\|\nabla\phi_2\|} \\ &= |f| ((u_1 \cdot t) - (u_2 \cdot t)) \text{ because } t \cdot n_1 = t \cdot n_2 = 0 \\ &= 0 \end{aligned}$$

because $u_1 \cdot t = u_2 \cdot t$ since $u = \nabla f$ with f piecewise linear and continuous on the face f , and $t \parallel f$.

2.2 Dimensionality and topology

We choose the tetrahedral mesh \mathcal{M} such that it is homotopy-equivalent to the 0 level set S_0 . In particular, they have the same Euler characteristic $\chi = 2 - 2g = |\mathcal{V}| - |\mathcal{E}| + |\mathcal{F}| - |\mathcal{T}|$. This is to ensure that the harmonic space on the implicit surface and the 3D harmonic space we will compute have the same dimension ($2g$).

We write \mathcal{F}^i the internal faces (i.e. the ones that are shared by two tetrahedra) of \mathcal{M} , and \mathcal{F}^b the faces of the boundary ($\mathcal{F} = \mathcal{F}^i \sqcup \mathcal{F}^b$). The distinction is important the curl operators are towards \mathcal{F}^i . Similarly we write \mathcal{E}^b the edges of the boundary.

As in Section 1, we can try to find a relation that will help us to get a robust decomposition where spaces have consistent dimensions. We have the following relations:

$$\begin{aligned} 4|\mathcal{T}| &= 2|\mathcal{F}| - |\mathcal{F}^b| && \mathcal{M} \text{ is a tetrahedral mesh} \\ |\mathcal{V}| - |\mathcal{E}| + |\mathcal{F}| - |\mathcal{T}| &= 2 - 2g && \text{Euler characteristic of } \mathcal{M} \\ 3|\mathcal{F}^b| &= 2|\mathcal{E}^b| && \text{The boundary of } \mathcal{M} \text{ is a triangular mesh} \\ |\mathcal{V}^b| - |\mathcal{E}^b| + |\mathcal{F}^b| &= 2(2 - 2g) && \text{Euler characteristic of the boundary of } \mathcal{M} \\ &&& (\text{two surfaces of genus } g) \end{aligned}$$

However, it seems that those equalities are not sufficient to get a relation like in Section 1.

This is why we try another approach using the dimensionality of the spaces associated with \mathcal{M}^0 . More precisely, we construct operators that extrapolate – in some consistent way – fields on the surface mesh \mathcal{M}^0 to fields over the ambient mesh \mathcal{M} . We then use those extrapolators to find the parts of the decomposition with least square formulation.

2.3 Decomposition

2.3.1 Curl-free part

Let $B_{\mathcal{V}}$ be the interpolator containing the barycentric coordinates, giving f^0 on the 0 level set from f on the ambient vertices (level set vertices of \mathcal{V}^0 are on the segment between two ambient vertices in \mathcal{V}). We would like to extrapolate f from f^0 (i.e. $B_{\mathcal{V}}f = f^0$) with Gf being as orthogonal to $\nabla\phi$ as possible (or equivalently, the projected gradient $\Pi_{\phi}Gf$ is as close as possible to the gradient Gf):

$$f = \arg \min \quad \|\sqrt{M_{\mathcal{T}}}(\Pi_{\phi}Gf - Gf)\|_2 \\ \text{s.t.} \quad B_{\mathcal{V}}f = f^0$$

This problem being over-constrained, we rather solve the following least squares problem:

$$f = \arg \min \|\sqrt{M_{\mathcal{T}}^*}(\Pi_{\phi}Gf - Gf)\|_2 + \lambda \|B_{\mathcal{V}}f - f^0\|_2 \\ = \arg \min \|A_{\mathcal{V}}f - b_{\mathcal{V}}\|_2$$

where $M_{\mathcal{T}}^*$ is the normalized mass matrix, with the sum of the diagonal equal to 1.

$$A_{\mathcal{V}} = \begin{pmatrix} \sqrt{M_{\mathcal{T}}^*}(\Pi_{\phi}Gf - Gf) \\ \sqrt{\lambda}B_{\mathcal{V}} \end{pmatrix} \quad b_{\mathcal{V}} = \begin{pmatrix} 0 \\ \sqrt{\lambda}f^0 \end{pmatrix}$$

The solution to this least squares problem is (see [Ame85] for the expression of the solution of a linearly constrained least-square problem):

$$f = \underbrace{\lambda(A_{\mathcal{V}}^\top A_{\mathcal{V}})^{-1}B_{\mathcal{V}}^\top}_{\Lambda_{\mathcal{V}}} f^0$$

Eventually, the curl-free part in the Helmholtz-Hodge decomposition v is given by the solution of the following least squares problem:

$$\Pi_{\phi}G\Lambda_{\mathcal{V}}f_*^0 \quad \text{where} \quad f_*^0 = \arg \min_{f^0 \in \mathcal{V}^0} \|\Pi_{\phi}G\Lambda_{\mathcal{V}}f^0 - v\|_2$$

Remark. Inspired by the closest point method (see [RM08, KSA⁺23]) that solves a surfacic PDE by embedding it in a tubular ambient neighborhood of the surface, I have also tried another extrapolator $\Lambda_{\mathcal{V}}$ that for any ambient $\mathbf{x} \in \mathcal{V}$ interpolates (with inverse distance weighting) the value on the k nearest neighbors of \mathbf{x} in \mathcal{V}_0 . It works as well but would be difficult to use it similarly for the divergence-free part.

2.3.2 Divergence-free part

The divergence-free part is trickier to deal with. The fact that the dual of the curl defined with finite volumes coincides with the rotated gradient, which was true in 2D (i.e. $M_{\mathcal{F}^0}^{-1}C_0^\top = JG_{\mathcal{E}^0}$, see Section 1.1), does not stand here (i.e. $M_{\mathcal{T}}^{-1}C_\phi^\top \neq JG_{\mathcal{F}}$). In fact, the face-based values are "abstract" and have no intuitive values contrary to the edge potential in 2D, and it would be nonsense to try to extrapolate from an edge potential to midface values. Therefore, we use an intermediary corner-based space (a value at each corner of each tetrahedron, without requiring continuity at vertices).

We write $g^0 \in \mathcal{E}^0$ an edge-based potential on the 0 level set, $g^{\mathcal{F}} \in \mathcal{F}^i$ a faced-based ambient potential, and $g^{\mathcal{C}} \in 4\mathcal{T}$ a corner-based ambient potential. Let also $B_{\mathcal{F}}$ containing the barycentric coordinates that permits to interpolate g^0 on the level set from the corner-based ambient $g^{\mathcal{C}}$ (level set edges of \mathcal{E}^0 are either on the triangle between three ambient vertices in \mathcal{V} associated with six corners, or inside a tetrahedron associated with four corners).

We will use a constraint to favour the continuity at vertices of $g^{\mathcal{C}}$, by defining the continuity operator $K : 4\mathcal{T} \rightarrow \underbrace{\bigoplus_{v \in \mathcal{V}} \mathcal{P}_2(\mathcal{N}(v))}_{\kappa}$ (where $\mathcal{P}_2(\mathcal{N}(v))$ is the space spanned by the pairs of corners associated with a vertex $v \in \mathcal{V}$) simply mapping any two neighboring corners into their difference:

$$(Kg^{\mathcal{C}})_{|(c_1, c_2)} = g_{c_1}^{\mathcal{C}} - g_{c_2}^{\mathcal{C}}$$

Having $Kg^{\mathcal{C}} = 0$ means that $g^{\mathcal{C}}$ is continuous. We can use with K the metric $M_{\mathcal{C}}$ containing for each $c \sim (v \in \mathcal{V}, t \in \mathcal{T})$ the volume of the Voronoi cells associated with v intersected with t .

This time, we want to have a corner-based ambient potential $g^{\mathcal{C}}$ that is as continuous as possible, such that the interpolation gives back the level set potential g^0 , and whose rotated gradient is the curl's dual applied on the face-based potential $g^{\mathcal{F}}$. Expressed as a minimization problem:

$$\begin{aligned} \arg \min_{(g^{\mathcal{C}}, g^{\mathcal{F}})} & \| \sqrt{M_{\mathcal{C}}} K g^{\mathcal{C}} \|_2 \\ \text{s.t. } & JG_{\mathcal{C}} g^{\mathcal{C}} = M_{\mathcal{T}}^{-1} C_\phi^\top g^{\mathcal{F}} \\ & B_{\mathcal{F}} g^{\mathcal{C}} = g^0 \end{aligned}$$

that is

$$\begin{aligned} \arg \min_{(g^{\mathcal{C}}, g^{\mathcal{F}})} & \| \sqrt{M_{\mathcal{C}}} K g^{\mathcal{C}} \|_2 \\ \text{s.t. } & \underbrace{\begin{pmatrix} JG_{\mathcal{C}} & -M_{\mathcal{T}}^{-1} C_\phi^\top \\ B_{\mathcal{F}} & 0 \end{pmatrix}}_{A_{\mathcal{F}} : 4\mathcal{T} \oplus \mathcal{F}^i \rightarrow 3\mathcal{T} \oplus \mathcal{E}^0} \cdot \underbrace{\begin{pmatrix} g^{\mathcal{C}} \\ g^{\mathcal{F}} \end{pmatrix}}_{b_{\mathcal{F}}} = \underbrace{\begin{pmatrix} 0 \\ g^0 \end{pmatrix}}_{b_{\mathcal{F}}} \end{aligned}$$

that is

$$\begin{aligned} \arg \min_{g=(g^{\mathcal{C}}, g^{\mathcal{F}})} & \| \tilde{K} g \|_2 \text{ with } \tilde{K} = \begin{pmatrix} \sqrt{M_{\mathcal{C}}} K & 0 \\ 0 & 0 \end{pmatrix} \\ \text{s.t. } & A_{\mathcal{F}} g = b_{\mathcal{F}} \end{aligned}$$

Unfortunately, \tilde{K} is singular and we have to use the following result to solve this problem.

Theorem (Linear equality constrained least-squares, [Ame85]). *Consider the following linearly constrained least-squares problem:*

$$\begin{aligned} \arg \min_{\beta} & \| X\beta - y \|_2 \\ \text{s.t. } & Q^\top \beta = c \end{aligned}$$

Let R such that $(Q \quad R)$ is non-singular and such that $R^\top Q = 0$. Then the estimator is:

$$\bar{\beta} = R(R^\top X^\top X R)^{-1} R^\top X^\top y + (I_p - R(R^\top X^\top X R)^{-1} R^\top X^\top X) Q(Q^\top Q)^{-1} c.$$

Let $p = 4|\mathcal{T}| + |\mathcal{F}^i|$ and $q = 3|\mathcal{T}| + |\mathcal{E}^0|$ so that $A_{\mathcal{F}}$ is a $q \times p$ constraint matrix. Let $\mathcal{L}_{\mathcal{C}} = \tilde{K}^\top \tilde{K}$, and R a $p \times (p - q)$ matrix spanning $\ker A_{\mathcal{F}}$ (so that $A_{\mathcal{F}}R = 0$ i.e. $R^\top A_{\mathcal{F}}^\top = 0$; and $(A_{\mathcal{F}} \quad R^\top)$ is a $p \times p$ non-singular matrix). This gives as a solution of our problem:

$$\begin{pmatrix} g^{\mathcal{C}} \\ g^{\mathcal{F}} \end{pmatrix} = (I_p - R(R^\top \mathcal{L}_{\mathcal{C}} R)^{-1} R^\top \mathcal{L}_{\mathcal{C}}) A_{\mathcal{F}}^\top (A_{\mathcal{F}} A_{\mathcal{F}}^\top)^{-1} b_{\mathcal{F}}$$

Now let

$$\Lambda_{\mathcal{F}} = (0 \quad I_{|\mathcal{F}^i|}) (I_p - R(R^\top \mathcal{L}_{\mathcal{C}} R)^{-1} R^\top \mathcal{L}_{\mathcal{C}}) A_{\mathcal{F}}^\top (A_{\mathcal{F}} A_{\mathcal{F}}^\top)^{-1} \begin{pmatrix} 0 \\ I_{|\mathcal{E}^0|} \end{pmatrix}$$

so that we have $g^{\mathcal{F}} = \Lambda_{\mathcal{F}} g_0$.

Eventually, as for the curl-free part, the divergent-free part of the decomposition of v is given by the solution of the following least squares problem:

$$M_{\mathcal{T}}^{-1} C_\phi^\top \Lambda_{\mathcal{F}} g_*^0 \quad \text{where} \quad g_*^0 = \arg \min_{g^0 \in \mathcal{E}^0} \|M_{\mathcal{T}}^{-1} C_\phi^\top \Lambda_{\mathcal{F}} g^0 - v\|_2$$

2.3.3 Harmonic part

In order to find the harmonic part of the decomposition, we first define two harmonic operators. The first one is on the level set:

$$H_2 = \begin{pmatrix} \Lambda_{\mathcal{V}}^\top G_\phi^\top M_{\mathcal{T}} \\ \Lambda_{\mathcal{F}}^\top C_\phi \\ \perp_\phi \end{pmatrix} : 3\mathcal{T} \rightarrow \mathcal{V}^0 \oplus \mathcal{E}^0 \oplus \mathcal{T}$$

where $(\perp_\phi u)_f = u_f \cdot n_f$ i.e. $\perp_\phi u = 0$ if and only if u is a tangential vector field. The other harmonic operator is in the ambient space:

$$H_3 = \begin{pmatrix} G^\top M_{\mathcal{T}} \\ C_3 \end{pmatrix} : 3\mathcal{T} \rightarrow \mathcal{V} \oplus 3\mathcal{F}^i$$

Let also M_H be the following metric for the 3D harmonic operator H_3 :

$$M_H = \begin{pmatrix} M_{\mathcal{V}}^{-1} & 0 \\ 0 & M_{\mathcal{F}^i}^{-1} \end{pmatrix}$$

Now, the idea is to find the subspace \mathcal{H} of $\mathcal{H}_2 = \ker H_2$ of dimension $2g$ that is – in an intuitive way – the closest of being in $\mathcal{H}_3 = \ker H_3$. Let $B_{\mathcal{H}_2}$ a basis of \mathcal{H}_2 . A basis $B_{\mathcal{H}}$ of \mathcal{H} is constructed as the $2g$ columns vectors v of $B_{\mathcal{H}_2}$ that have the lowest value $h^\top \mathcal{L}_H h$:

$$B_{\mathcal{H}} = 2g \cdot \arg \min_{h \in B_{\mathcal{H}_2}} \|h^\top \mathcal{L}_H h\|_2 \quad \text{with } \mathcal{L}_H = (H_3)^\top M_H H_3.$$

The harmonic space $\mathcal{H} = \text{Span } B_{\mathcal{H}}$ has by construction the correct dimension $2g$. We can recover the harmonic remainder of the decomposition by solving the following least squares problem:

$$B_{\mathcal{H}} c_* \quad \text{where} \quad c_* = \arg \min_{c \in \mathbb{R}^{2g}} \|B_{\mathcal{H}} c - v\|_2$$

Harmonicity By design, for any $h \in \mathcal{H}$, $h \in \ker(\Lambda_{\mathcal{V}}^\top G_\phi^\top M_{\mathcal{T}}) \cap \ker(\Lambda_{\mathcal{F}}^\top C_\phi) \cap \ker(\perp_\phi)$. $\ker \Lambda_{\mathcal{V}}^\top$ is of dimension 1 containing scalar fields that are constant on level sets, and since h is tangential ($\perp_\phi h = 0$), $G_\phi^\top M_{\mathcal{T}} h$ is constant along the normals, so we have $G_\phi^\top M_{\mathcal{T}} h = 0$. In addition in practice $\Lambda_{\mathcal{F}}^\top$ is injective so $C_\phi h = 0$. Therefore $G_\phi^\top M_{\mathcal{T}} h = D_\phi h = 0$ (divergent-free) and $C_\phi h = 0$ (curl-free), which is what we want for an harmonic field. In the experiments, this is verified up to the numerical precision.

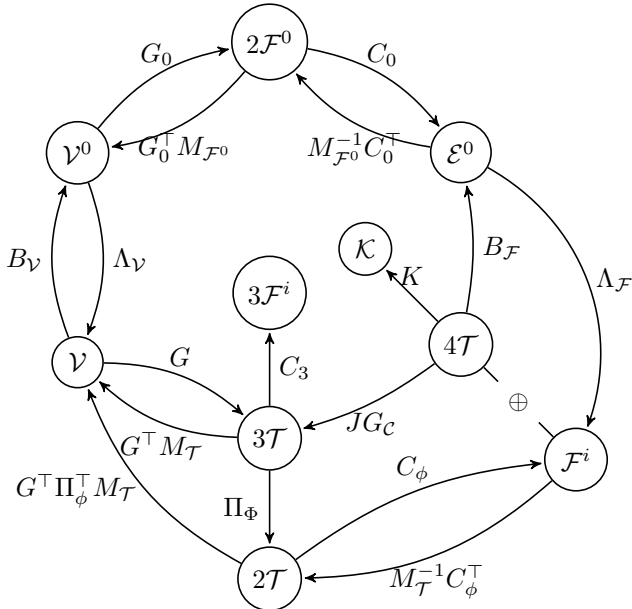


Figure 4: Graphic summary of the spaces and operators between them defined in the section.

2.4 Robustness

With the above method, we can consider we are using the following "extrapolating" differential operators:

$$\begin{aligned}\tilde{G} &= G_\phi \Lambda_V \\ \widetilde{JG} &= M_T^{-1} C_\phi^\top \Lambda_F \\ \widetilde{D} &= \widetilde{G}^\top M_T = \Lambda_V^\top G_\phi^\top M_T \\ \widetilde{C} &= \widetilde{JG}^\top M_T = \Lambda_F^\top C_\phi\end{aligned}$$

Using the fact that $C_\phi G_\phi = 0$ (Section 2.1), we can check that the following structural identities are verified:

$$\begin{aligned}\widetilde{C}\widetilde{G} &= 0 \\ \widetilde{D}\widetilde{JG} &= 0\end{aligned}$$

Eventually we can use them (and the fact that $\mathcal{H} \subset \ker \widetilde{D} \cap \ker \widetilde{C}$) to show that we have the direct sum:

$$\text{Im } \widetilde{G} \oplus \text{Im } \widetilde{JG} \oplus \mathcal{H}.$$

2.5 Results

Figures 5, 6, 7 shows the Helmholtz-Hodge decomposition obtained with the above method on the implicit function of a sphere (genus 0, Figure 5), a torus (genus 1, Figure 6), and a "tetrahedron wireframe" (genus 3, Figure 7).

One application that I have tested is the harmonic completion of a tangent vector field, using the previous computation of the harmonic space \mathcal{H} . For instance, in the case of the torus, a single tangent vector in the ambient space suffices to define a whole harmonic field (since in this case the harmonic space is of dimension 2). If the harmonic space is already computed, this kind of completion is extremely fast because it only needs the resolution of a $2g \times 2g$ linear system (if g vectors provided) or a $2g \times 2n$ least squares problem (if $n > g$ vectors provided).

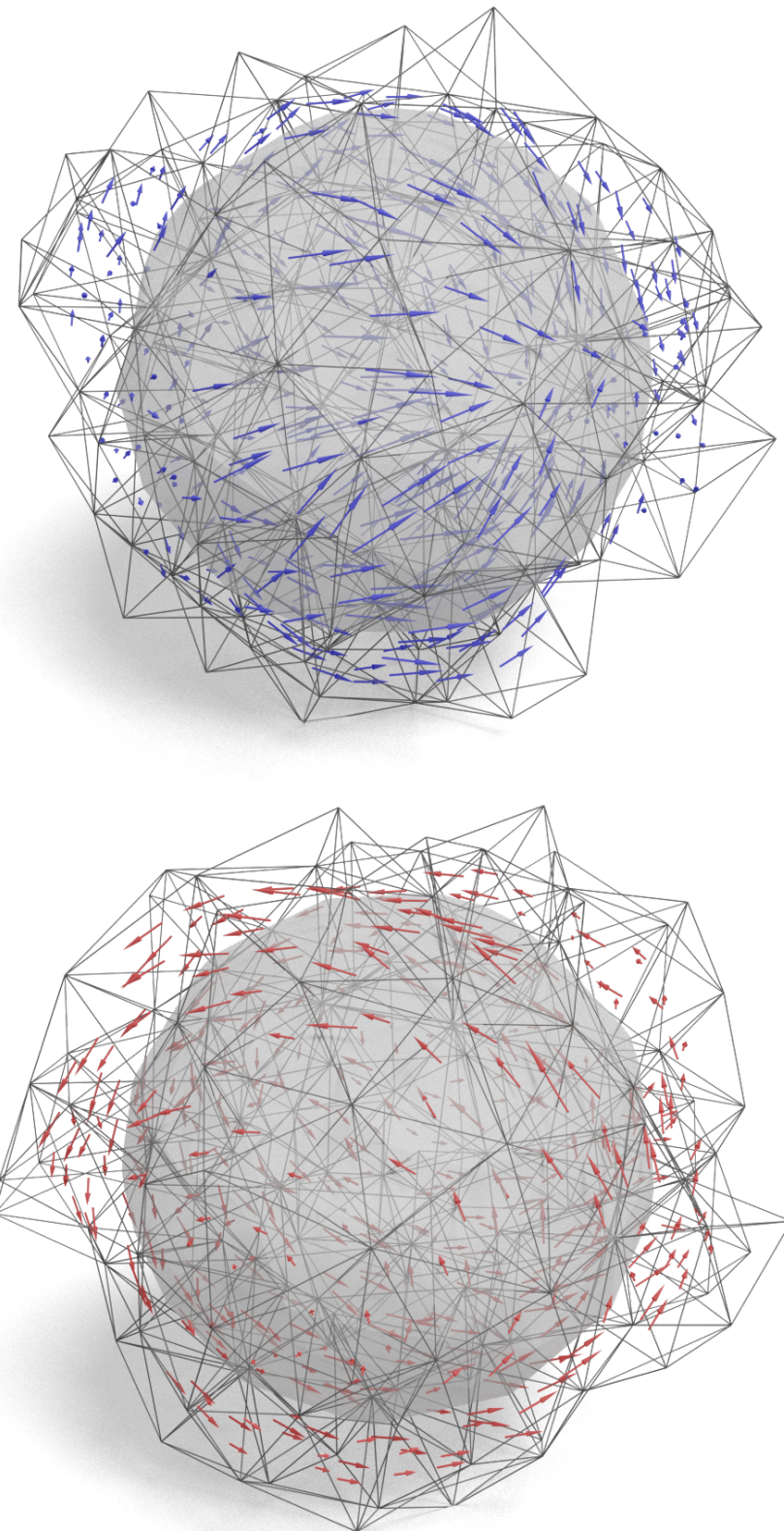


Figure 5: Decomposition using our method on an implicit sphere. Top: curl-free part (blue); bottom: divergent-free part (red). The harmonic part is, as expected, null because the sphere is of genus 0. The tetrahedra set \mathcal{T} is shown in wire-frame, and the grey, transparent surface is the mesh \mathcal{M}^0 .

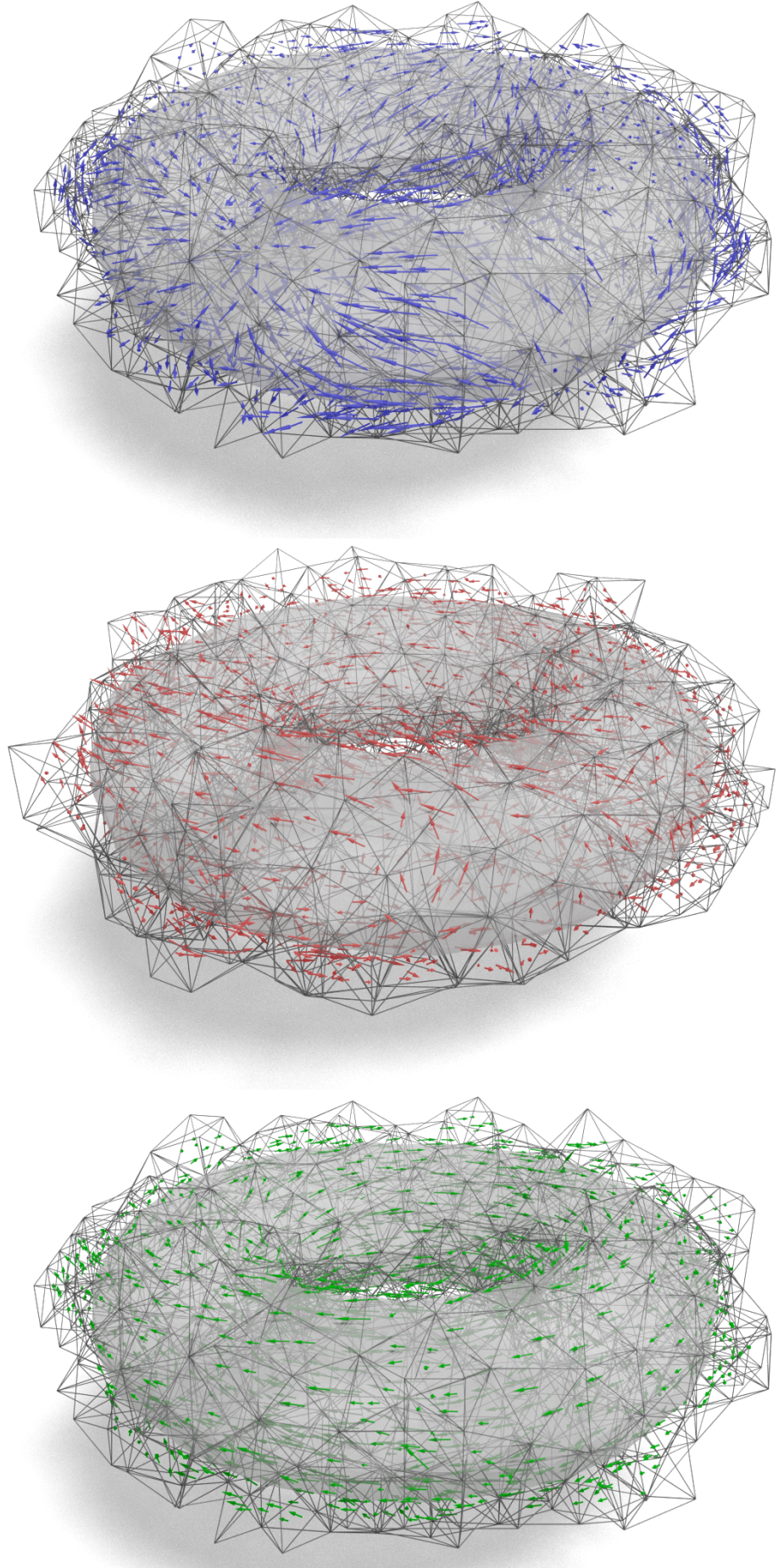


Figure 6: Decomposition using our method on an implicit torus. Top: curl-free part (blue); middle: divergent-free part (red); bottom: harmonic part (green). The tetrahedra set \mathcal{T} is shown in wire-frame, and the grey, transparent surface is the mesh \mathcal{M}^0 .

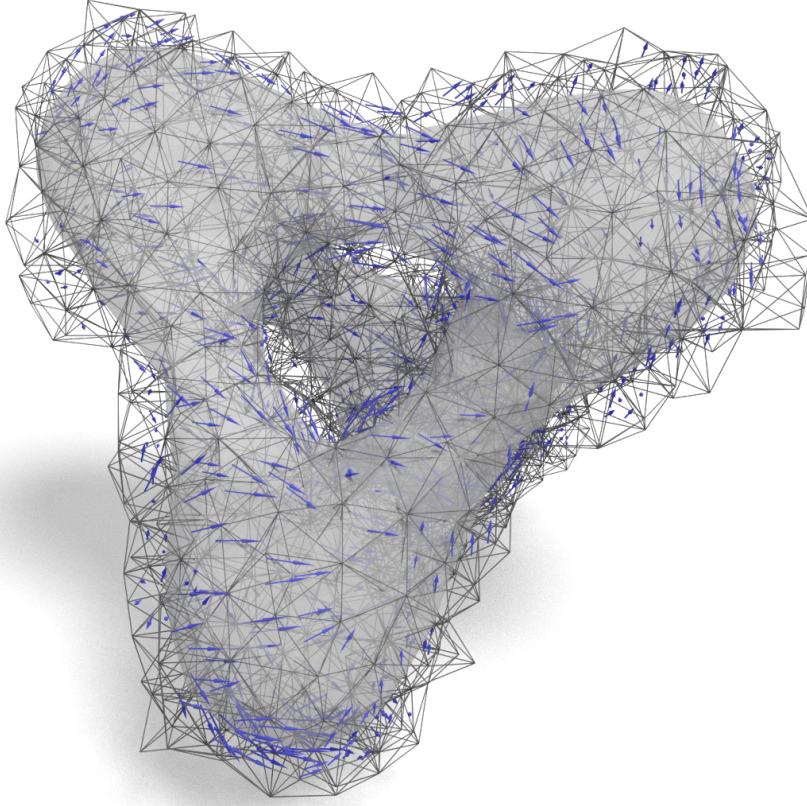


Figure 7: Curl-free part computed on a implicit function given by: $\phi(x) = d(x, T_0)d(x, T_1)$ where T_0 and T_1 are respectively the 4 vertices and the geometric edges of a regular tetrahedron. The shown iso-surface S_c for some $c > 0$ has genus 3. The relatively high number of tetrahedra (more than 3000) necessary to obtain the right topology makes computationally difficult to obtain the divergent-free and the harmonic parts.

References

- [Ame85] Takeshi Amemiya. *Advanced econometrics*. Harvard university press, 1985.
- [BV22] Iwan Boksebeld and Amir Vaxman. High-order directional fields. *ACM Transactions on Graphics (TOG)*, 41(6):1–17, 2022.
- [CL93] Brian Cabral and Leith Casey Leedom. Imaging vector fields using line integral convolution. In *Proceedings of the 20th annual conference on Computer graphics and interactive techniques*, pages 263–270, 1993.
- [DGDT16] Fernando De Goes, Mathieu Desbrun, and Yiying Tong. Vector field processing on triangle meshes. In *ACM SIGGRAPH 2016 Courses*, pages 1–49. 2016.
- [KSA⁺23] Nathan King, Haozhe Su, Mridul Aanjaneya, Steven Ruuth, and Christopher Batty. A closest point method for surface pdes with interior boundary conditions for geometry processing. *arXiv preprint arXiv:2305.04711*, 2023.
- [PP03] Konrad Polthier and Eike Preuß. Identifying vector field singularities using a discrete hodge decomposition. In *Visualization and mathematics III*, pages 113–134. Springer, 2003.
- [RM08] Steven J Ruuth and Barry Merriman. A simple embedding method for solving partial differential equations on surfaces. *Journal of Computational Physics*, 227(3):1943–1961, 2008.